IEEE Access
Multidisciplinary | Rapid Review | Open Access Journal

Received March 17, 2019, accepted April 5, 2019, date of publication April 17, 2019, date of current version April 26, 2019.

Digital Object Identifier 10.1109/ACCESS.2019.2910725

Robust Internal-Loop Compensator Based Sliding Mode Control of Nonlinear Systems in the Presence of Mismatched Disturbances

ALMIR SALIHBEGOVIC, (Member, IEEE)
Department for Automatic Control and Electronics, Faculty of Electrical Engineering, University of Sarajevo, 71000 Sarajevo, Bosnia and Herzegovina
e-mail: almir.salihbbegovic@etf.unsa.ba

ABSTRACT This paper introduces the robust internal-loop compensator based sliding mode control (SMRIC) scheme for multiple-input multiple-output (MIMO) nonlinear systems subjected to mismatched uncertainties, which are time-varying and non-vanishing with non-constant steady-state values. The proposed approach extends an application area of the robust internal-loop compensator (RIC), as well as a class of mismatched uncertainties that could be imposed on the system. The developed SMRIC technique allows substantial alleviation of the chattering phenomenon in the presence of disturbances while retaining the nominal performance of the system in the absence of disturbances. The stability analysis of the closed-loop system is performed using the Lyapunov-based approach. The proposed SMRIC method guarantees the finite-time convergence of the system trajectories to the sliding surface and provides asymptotic stability of the equilibrium. The simulation results of the numerical example and both simulation and experimental results of the application example show that the proposed SMRIC technique exhibits, in comparison with the concurrent algorithms, excellent tracking performance and robustness properties in the presence of modeling uncertainties, parameter variations, external disturbances, and mismatched uncertainties.

INDEX TERMS Control design, control system synthesis, disturbance observer, Lyapunov methods, motion control, nonlinear control systems, observers, sliding mode control, stability analysis, uncertain systems.

I. INTRODUCTION

Due to a conceptual simplicity and a good performance, the sliding mode control (SMC) has been widely used technique in industrial applications for a robust compensation of matched disturbances using the concepts of sliding modes (SMs) and the equivalent control [1]–[3]. Many theoretical aspects of the variable structure systems (VSSs) with SMs have been described in the survey papers [3]–[6], such as a chattering phenomenon due to a discontinuous control [7], a nominal performance recovery [8], and an insensitivity to the matching disturbances, where the disturbance relative degree (DRD) is not less than the input relative degree (IRD). It is noticed that most approaches to the sliding surface design are focused to the matched disturbances compensation [9]–[14]. However, mismatched (unmatched) disturbances (uncertainties) exist in many practical applications, such as motion control systems [15], and flight control systems [16], in which the lumped disturbance torque, caused by wind gusts, parameter variations and modeling uncertainties, always affects the system states directly, rather than through the control input channels. Therefore, different authors [17]–[20] have focused to the sliding surface design for nonlinear systems subjected to mismatched disturbances that are vanishing (H_2 norm bounded) or with constant-steady state values. In these approaches, a chattering attenuation and recovery of a nominal control performance are still severe problems to be solved. Indeed, baseline SMC techniques, such as integral SMC (I-SMC) [20], [21], terminal SMC (T-SMC) [22] or higher order SMC (HO-SMC) [23]), attenuate mismatched uncertainties directly by increasing the magnitude of the switching control term, which results in a enlarged chattering. Significant chattering can cause loss of the system nominal performance in the absence of disturbances. By exploiting the disturbance observers (DOBs) with the SMC framework, the switching magnitudes are significantly reduced to compensate only the disturbance compensation error, instead of the whole disturbance. To this end, many papers have reported DOB based SMC schemes for linear systems sub-

The associate editor coordinating the review of this manuscript and approving it for publication was Bing Li.

jected to a large class of unmatched disturbances [24], [25]. DOB based robust control techniques [8], [15], [26]–[28] are extended to a class of nonlinear systems in the presence of mismatched uncertainties. The widely used NDOB based SMC [15] has been recognized in the academic community as outstanding and particularly significant among others (N)DOB based robust control techniques. Nevertheless, mismatched disturbances are assumed to have constant-steady state values (or equivalently, the first order time derivative of these disturbances is supposed to be zero in a steady-state), and the first order time derivative of these uncertainties is supposed to be bounded in the NDOB based SMC approach [15]. The relaxed assumptions imposed on mismatched disturbances have been reported in [29], in which the authors assumed that disturbances have to be continuous. However, these assumptions imposed on unmatched uncertainties are strong and do not represent reasonable assumptions for many practical engineering systems. For example, wind gusts in flight (motion) control systems are bounded disturbances that do not have to be continuous, or with constant steady-state values.

On the other hand, the linear robust internal-loop compensator (RIC) [30]–[36] has been introduced as a generalized framework for uncertainties attenuation of linear systems, in order to ensure the unified disturbance compensation analysis of different control strategies, such as the DOB based control (DOBC) and the adaptive robust control (ARC). It also provides a quantified trade-off between two major requirements in a robust control design: (a) robustness properties to various uncertainties, and (b) desired performance of the closed-loop system. However, the RIC stability analysis is originally presented only for linear systems [30]–[36]. By synthesizing the RIC framework with Lyapunov based redesign, the RIC based I-SMC method is introduced for single-input, single-output (SISO) [37] and MIMO [38] electromechanical systems, ensuring the finite-time convergence of the system trajectories to the particular sliding surface, as well as the uniformly ultimate boundedness of the system solutions.

This paper proposes the novel SMRIC method for a class of MIMO electromechanical systems in the presence of mismatched disturbances, which are time-varying and non-vanishing with non-constant steady state values. The contributions of the proposed SMRIC method are:

1) It alleviates the chattering phenomenon of MIMO electromechanical systems subjected to a large class of mismatched disturbances, by requiring the magnitudes of the switching control term to be larger only than the bound of the disturbance compensation error, rather than that of the lumped disturbance,
2) It retains a nominal control performance of MIMO electromechanical systems, since the RIC serves like a patch to the baseline controller that does not operate in the absence of disturbances,
3) It extends an application area of the RIC scheme for stability analysis of MIMO electromechanical systems subjected to mismatched disturbances, since the RIC stability analysis is originally introduced only for a class of linear systems [30]–[36],
4) It is proposed for a class of MIMO nonlinear systems, unlike the concurrent NDOB based SMC [15] that is introduced for a class of SISO nonlinear systems,
5) It expands a class of mismatched uncertainties that could be imposed on MIMO electromechanical systems, requiring only the knowledge about the boundedness of disturbances. Therefore,
   a) Unlike the NDOB based SMC [15], it does not require constant steady-state values of the mismatched uncertainties for stabilization of the DOB (for example, wind gusts in flight control systems are bounded disturbances that do not have constant steady-state values), and
   b) Unlike the extended DOB based SMC [29], it does not require mismatched disturbances to be continuous (for example, wind gusts in motion control systems are bounded disturbances that do not have to be continuous),
6) It exhibits significant tracking performance of the application example in comparison with the NDOB based SMC [15], as well as improved robustness to the modeling uncertainties, parameter variations, external disturbances and mismatched uncertainties, even in the scenario with the same values of the switching control term.

Furthermore, the following extensions of our previous work [37]–[40] are presented:

1) The proposed SMRIC method aims to solve the disturbance compensation problem for nonlinear MIMO systems with arbitrary DRDs (matched and mismatched disturbances),
2) The generalized sliding surface (not particular one, as in [37]–[40]) is utilized in the SMRIC framework,
3) Stronger results in stability analysis are proved, ensuring the finite-time convergence of the system trajectories to the generalized sliding manifold, as well as the asymptotic stability of the equilibrium, and
4) The RIC based phase-lead compensator is utilized, through the SMRIC framework, for attenuation of additional disturbances in the application example, thus increasing the stability margins and decreasing settling times of the closed loop system.

The paper is structured as follows. Section II introduces the typical MIMO numerical example in order to illustrate susceptibility of the baseline I-SMC (without DOB) and baseline NDOBC (without SMC) [8] methods, as well as insensitivity of the NDOB based I-SMC [15] and the RIC based I-SMC [38] techniques to time-varying and non-vanishing mismatched disturbances. In Section III the unified SMRIC method is proposed for a class of MIMO nonlinear electromechanical systems using Lyapunov based redesign. The summary model of the application example and the control design are reported in Section IV. The effectiveness of the

proposed SMRIC technique is demonstrated through both the simulation studies and the experimental tests in Section V, using the small-scale helicopter CE 150 in the presence of modeling uncertainties, parameter variations, wind gusts and dynamical changes in the center of gravity (CoG). Finally, the last section concludes the paper.

II. A MOTIVATIONAL EXAMPLE

This section describes the typical MIMO numerical example [8] subjected to mismatched disturbances, in order to show superior tracking performance of the RIC based I-SMC method [38] in compensation of mismatched disturbances, which are time-varying and non-vanishing with non-constant steady-state values. Furthermore, comparison analysis with the concurrent control methods for mismatched uncertainties compensation is presented.

Consider the MIMO nonlinear system with mismatched disturbances $w_1(t)$ and $w_2(t)$ [8]

$$\begin{cases} \dot{x}_1 = -x_1 + x_1x_2 + x_3 + w_1, \\ \dot{x}_2 = \sin x_1 + x_2^2 + x_4 + w_2, \\ \dot{x}_3 = x_4 + u_1, \\ \dot{x}_4 = u_2, \\ y_1 = x_1, \\ y_2 = x_2, \end{cases} \tag{1}$$

where x_1, x_2, x_3 and x_4 are system states, u_1 and u_2 denote control inputs, while y_1 and y_2 represent system outputs. The IRDs $(\varrho_1, \varrho_2) = (2, 2)$ for the system (1) are greater than the DRDs $(\vartheta_1, \vartheta_2) = (1, 1)$. Thus the disturbances w_1 and w_2 do not satisfy the matching condition, or in other words, the disturbances w_1 and w_2 act on the system (1) via different channels than the control inputs u_1 and u_2.

Consider the time-varying and non-vanishing mismatched uncertainties $w_1(t)$ and $w_2(t)$ with non-constant steady state values

$$w_1(t) = \begin{cases} 0, & t \in [0, 4) \\ 2, & t \in [4, 8) \\ \frac{3}{5}\sin\left(\frac{\pi}{2}t\right) + 2, & t \in [8, +\infty) \end{cases} \tag{2}$$

and

$$w_2(t) = \begin{cases} 0, & t \in [0, 4) \\ -3, & t \in [4, 8) \\ -\frac{4}{5}\sin\left(\pi t + \frac{\pi}{2}\right) - 3, & t \in [8, +\infty). \end{cases} \tag{3}$$

to be imposed on the system (1) in order to compare disturbance attenuation characteristics of the following control algorithms: the baseline NDOBC (without SMC) technique [8], the NDOB based I-SMC scheme [15], the baseline I-SMC (without DOB) [15], [38] and the RIC based I-SMC method [38].

Let $x = [x_1, x_2, x_3, x_4]^T$, $u = [u_1, u_2]^T$, $w = [w_1, w_2]^T$ and $y = [y_1, y_2]^T$ then the system (1) can be expressed in the matrix form as

$$\begin{cases} \dot{x} = f(x) + g(x)u + p(x)w, \\ y = h(x), \end{cases} \tag{4}$$

where the matrix fields $f(x)$, $g(x)$, $p(x)$ and $h(x)$ are

$$f(x) = \begin{bmatrix} f_1(x) \\ f_2(x) \\ f_3(x) \\ f_4(x) \end{bmatrix} = \begin{bmatrix} -x_1 + x_1x_2 + x_3 \\ \sin x_1 + x_2^2 + x_4 \\ x_4 \\ 0 \end{bmatrix}, \tag{5}$$

$$g(x) = \begin{bmatrix} g_1(x) \\ g_2(x) \end{bmatrix}^T = \begin{bmatrix} 0 & 0 & 1 & 0 \\ 0 & 0 & 0 & 1 \end{bmatrix}^T, \tag{6}$$

$$h(x) = \begin{bmatrix} h_1(x) \\ h_2(x) \end{bmatrix} = \begin{bmatrix} x_1 \\ x_2 \end{bmatrix}, \tag{7}$$

$$p(x) = \begin{bmatrix} p_1(x) \\ p_2(x) \end{bmatrix}^T = \begin{bmatrix} 1 & 0 & 0 & 0 \\ 0 & 1 & 0 & 0 \end{bmatrix}^T. \tag{8}$$

A. BASELINE NDOB CONTROL

The nonlinear disturbance observer (NDOB) is defined as [8]

$$\begin{cases} \hat{w} = z_w + \lambda(x), \\ \dot{z}_w = -l(x)\left[p(x)\left(\lambda(x) + z_w\right) + f(x) + g(x)u\right], \end{cases} \tag{9}$$

where $\hat{w} = [\hat{w}_1, \hat{w}_2]^T$ is the estimation vector of the disturbance vector w, $z_w = [z_{w1}, z_{w2}]^T$ represents the internal state vector of the NDOB, $\lambda = [\lambda_1, \lambda_2]^T$ is a vector of the observer functions selected as in [8], i.e. $\lambda = [50x_1, 50x_2]^T$, and the NDOB gain vector $l \in \mathbb{R}^{2\times 4}$ is

$$l(x) = \frac{\partial \lambda(x)}{\partial x} = \begin{bmatrix} 50 & 0 & 0 & 0 \\ 0 & 50 & 0 & 0 \end{bmatrix}. \tag{10}$$

The dynamics of the observer state vector z_w is derived using (9) and (10)

$$\dot{z}_w = \begin{bmatrix} \dot{z}_{w1} \\ \dot{z}_{w2} \end{bmatrix} = \begin{bmatrix} -50(50x_1 + z_{w1} + f_1) \\ -50(50x_2 + z_{w2} + f_2) \end{bmatrix}. \tag{11}$$

The NDOB based control law for the system (1) is defined as [8]

$$u(x) = A^{-1}(x)\left[-b(x) + v(x) + \Gamma(x)\hat{w}\right]. \tag{12}$$

Appropriate vector or matrix fields in (12) are derived using Lie derivatives as

$$A(x) = \begin{bmatrix} L_{g1}L_f h_1 & L_{g2}L_f h_1 \\ L_{g1}L_f h_2 & L_{g2}L_f h_2 \end{bmatrix} = \begin{bmatrix} 1 & 0 \\ 0 & 1 \end{bmatrix}, \tag{13}$$

$$b(x) = \begin{bmatrix} L_f^2 h_1 \\ L_f^2 h_2 \end{bmatrix} = \begin{bmatrix} (x_2 - 1)f_1 + x_1 f_2 + x_4 \\ f_1 \cos x_1 + 2x_2 f_2 \end{bmatrix}, \tag{14}$$

$$v(x) = \begin{bmatrix} -c_0^1 h_1 - c_1^1 L_f h_1 \\ -c_0^2 h_2 - c_1^2 L_f h_2 \end{bmatrix} = \begin{bmatrix} c_0^1(r_1 - x_1) - c_1^1 f_1 \\ c_0^2(r_2 - x_2) - c_1^2 f_2 \end{bmatrix}, \tag{15}$$

$$\Gamma(x) = \begin{bmatrix} -c_1^1 L_{p1} h_1 - L_{p1} L_f h_1 & -c_1^1 L_{p2} h_1 - L_{p2} L_f h_1 \\ -c_1^1 L_{p1} h_2 - L_{p1} L_f h_2 & -c_1^1 L_{p2} h_2 - L_{p2} L_f h_2 \end{bmatrix} = \begin{bmatrix} 1 - x_2 - c_1^1 & -x_1 \\ -\cos x_1 & -c_1^2 - 2x_2 \end{bmatrix}, \tag{16}$$

where c_0^1, c_1^1, c_0^2 and c_1^2 represent positive constants, while $r_1(t)$ and $r_2(t)$ stand for the reference signals.

B. NDOB BASED I-SMC

Define the integral sliding surface vector as [15]

$$\sigma = \begin{bmatrix} \sigma_1 \\ \sigma_2 \end{bmatrix} = \begin{bmatrix} \dot{e}_1 + c_1^1 e_1 + c_0^1 \int e_1 + \hat{w}_1 \\ \dot{e}_2 + c_1^2 e_2 + c_0^2 \int e_2 + \hat{w}_2 \end{bmatrix}, \tag{17}$$

where $e_1 = y_1 - r_1$ and $e_2 = y_2 - r_2$ are output tracking errors. The NDOB based I-SMC law is now defined as [15]

$$u(x) = A^{-1}(x)\left[-b(x) + v(x) + \Gamma(x)\hat{w} + v_{con}(x)\right], \tag{18}$$

where the corresponding control terms in (18) are the same with those in (12), and $v_{con} = [v_{con1}, v_{con2}]^T$ represents the convergence control vector

$$v_{con}(x) = \begin{bmatrix} -\beta_1 \operatorname{sgn} \sigma_1 \\ -\beta_2 \operatorname{sgn} \sigma_2 \end{bmatrix} \tag{19}$$

with positive coefficients β_1 and β_2.

C. BASELINE I-SMC

Define the integral sliding surface as [38]

$$\sigma = \begin{bmatrix} \sigma_1 \\ \sigma_2 \end{bmatrix} = \begin{bmatrix} \dot{e}_1 + c_1 e_1 + c_2 \int e_1 \\ \dot{e}_2 + c_3 e_2 + c_4 \int e_2 \end{bmatrix}, \tag{20}$$

where c_1, c_2, c_3, and c_4 are positive constants. The I-SMC vector is formulated as

$$u(x) = u_{eq}(x) + u_{con}(x), \tag{21}$$

where the equivalent control vector $u_{eq} = [u_{eq1}, u_{eq2}]^T$ is derived using (20) and $\dot{\sigma} = 0$ in the absence of disturbances, i.e. $w = 0$,

$$u_{eq}(x) = \begin{bmatrix} (1 - x_2 - c_1)f_1 - x_1 f_2 - x_4 - c_2 x_1 \\ -(c_3 + \cos x_1)f_1 - 2x_2 f_2 - c_4 x_2 \end{bmatrix} + \begin{bmatrix} \ddot{r}_1 + c_1 \dot{r}_1 + c_2 r_1 \\ \ddot{r}_2 + c_3 \dot{r}_2 + c_4 r_2 \end{bmatrix}. \tag{22}$$

The convergence control term u_{con} in (21) is designed as

$$u_{con}(x) = \begin{bmatrix} -\beta_1 \operatorname{sgn} \sigma_1 \\ -\beta_2 \operatorname{sgn} \sigma_2 \end{bmatrix}. \tag{23}$$

D. RIC BASED I-SMC

The RIC based I-SMC law [38] for the system (1) is designed as

$$u(x) = u_{eq}(x) + u_{con}(x) + u_{est}(x), \tag{24}$$

where the control vectors $u_{eq}(x)$ and $u_{con}(x)$ are defined the same as in the I-SMC algorithm (21). The estimation control term $u_{est}(x)$ is designed such that the RIC emulates the first-order low-pass filter in the DOB framework [34], [38]

$$u_{est}(x) = \begin{bmatrix} -(\eta_{11}\sigma_1 + \eta_{12}\sigma_2) \\ -(\eta_{21}\sigma_1 + \eta_{22}\sigma_2) \end{bmatrix}, \tag{25}$$

where the observer parameters η_{11}, η_{12}, η_{21} and η_{22} are positive coefficients representing the cut-off frequencies of the first-order filters, and the integral sliding surface σ is selected as in (20).

E. SIMULATION RESULTS

The control parameter values of the designed control laws for the system (1) are listed in Tab. 1. The same parameter values of the baseline I-SMC and the baseline NDOBC laws are used as in [8]. The authors in [8] used reference signals $r_1 = 10$ and $r_2 = 20$, but the magnitudes of these references are significant in comparison with the magnitudes of the tracking errors, so the disturbance compensation properties could not be easily noticed in the diagrams presented in [8]. Therefore, we present tracking performance of the control algorithms for the reference signals $r_1 = r_2 = 0$, in order to ensure better insight into the disturbance attenuation characteristics of the designed control schemes. It can be observed from Fig. 1a and Fig. 1b that the baseline I-SMC and NDOBC methods exhibit poor tracking performance in the presence of mismatched disturbances, revealing higher overshoots and settling times of the output variables. The baseline I-SMC and NDOBC techniques are capable to eliminate only the offset in the mismatched disturbances after the time instant $t = 8[s]$ at which the disturbances (2) and (3) start to vary in time. On the other hand, the simulation results confirmed that the RIC based I-SMC and the NDOB based I-SMC methods are able to handle mismatched disturbances in a robust way, retaining the nominal control performance, even within the time interval $t \in (4, 8)$, when the mismatched disturbances (2) and (3) reach the step changes, or within the time interval $t \in (4, 8)$ where w_1 and w_2 are time-varying and non-vanishing. Zoom areas in Fig. 1a and Fig. 1b show that the RIC based I-SMC law, in comparison with NDOB based I-SMC algorithm, slightly improved rise and settling times, as well as overshoots and undershoots after the time instant $t = 4[s]$ at which step changes of the disturbances occurred.

III. SMRIC FRAMEWORK FOR A CLASS OF MIMO ELECTROMECHANICAL SYSTEMS

This section presents the synthesis of the SMC and the RIC schemes, through Lyapunov redesign method, into the novel SMRIC framework for electromechanical MIMO systems. In comparison with the concurrent algorithms [15], [29], the proposed SMRIC method expands the class of mismatched disturbances that might be imposed on the system. Additionally, the stability analysis is derived for MIMO systems, unlike the NDOB based SMC [15], with stronger results in stability analysis as compared with the extended DOB based SMC [29].

The dynamics of the MIMO nonlinear electromechanical system can be described with [3], [41]

$$a(q)\ddot{q} + b(q, \dot{q}) + g(q) + \tau_d(t, q, \dot{q}) = \tau, \tag{26}$$

where $q(t) \in \mathbb{R}^n$ and $\dot{q}(t) \in \mathbb{R}^n$ represent a state vectors, position and velocity, respectively, $a(q) \in \mathbb{R}^{n \times n}$ is a non-singular positive definite matrix denoting an inertia of the system, $b(q, \dot{q}) \in \mathbb{R}^n$ represents a friction, centrifugal and Coriolis torques, $g(q) \in \mathbb{R}^n$ is a vector of gravitational torques, a disturbance vector $\tau_d(t, q, \dot{q}) \in \mathbb{R}^n$ may include various terms, such as interaction torques $\tau_{int} \in \mathbb{R}^n$ and

TABLE 1. Control parameters for the numerical example.

Controllers	Parameters
NDOBC	$c_0^1 = 20, c_1^1 = 9,$ $c_0^2 = 24, c_1^2 = 10,$ $\lambda_1(x) = x_1, \lambda_2(x) = x_2$
NDOB based I-SMC	$c_0^1 = 20, c_1^1 = 9,$ $c_0^2 = 24, c_1^2 = 10,$ $\beta_1 = \beta_2 = 50,$ $\lambda_1(x) = x_1, \lambda_2(x) = x_2$
I-SMC	$c_1 = 12, c_2 = 24,$ $c_3 = 20, c_4 = 34,$ $\beta_1 = \beta_2 = 50$
RIC based I-SMC	$c_1 = 12, c_2 = 24,$ $c_3 = 20, c_4 = 34,$ $\beta_1 = \beta_2 = 50,$ $\eta_{11} = \eta_{21} = 0.5,$ $\eta_{12} = \eta_{22} = 1$

external disturbances $\tau_{ext} \in \mathbb{R}^n$, while $\tau \in \mathbb{R}^n$ denotes a control input vector. The term torque will be used within the text, although the model (26) is valid for both rotational and translation motion. A perturbation of the system (26) yields

$$a_n\ddot{q} + \tau_{dis}(t, q, \dot{q}) = \tau, \tag{27}$$

where $a_n \in \mathbb{R}^{n\times n}$ is a non-singular positive definite matrix denoting a nominal inertia of the system, τ_{dis} represents a generalized (lumped) disturbance vector that may include different uncertain terms due to the model simplifications and parameter variations, as well as vectors $b(q, \dot{q})$, $g(q)$, and $\tau_d(t, q, \dot{q})$ from (26). We suppose that the vector functions b, g, τ_d and τ_{dis} are sufficiently smooth, and defined for $(q, \dot{q}, \tau) \in D \times D \times \mathbb{R}^n$, where $D \subset \mathbb{R}^n$ is a domain that contains the origin.

Remark 1: The model (26) or (27) allows a unified representation of various motion control tasks [3], such as position or velocity control, interaction torque control, etc. It is also suitable for description of nonlinear systems with mismatched disturbances. For example, the system (1) or (4) can be described with (27) by introducing the following substitutions: $a_n = diag(1, 1, 1, 1)$, $\dot{q} = x$, $\tau_{dis} = -f(x) - p(x)w$ and $\tau = g(x)u$, i.e.

$$a_n = \begin{bmatrix} 1 & 0 & 0 & 0 \\ 0 & 1 & 0 & 0 \\ 0 & 0 & 1 & 0 \\ 0 & 0 & 0 & 1 \end{bmatrix}, \quad \dot{q} = \begin{bmatrix} x_1 \\ x_2 \\ x_3 \\ x_4 \end{bmatrix}, \tag{28}$$

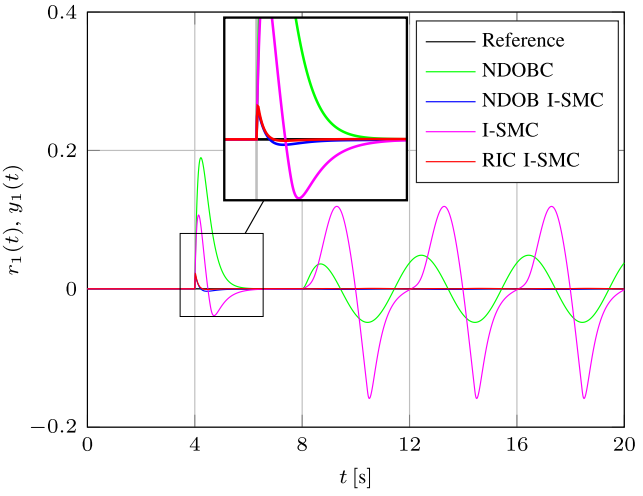

(a)

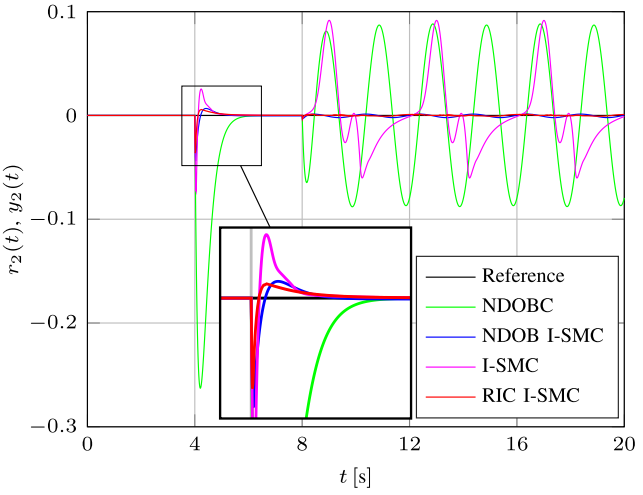

(b)

FIGURE 1. Output responses of the system (1) acquired by the control laws (12), (18), (21), and (24) in the presence of mismatched disturbances. (a) Comparison of the output y_1 responses. (b) Comparison of the output y_2 responses.

$$\tau_{dis} = \begin{bmatrix} x_1 - x_1x_2 - x_3 - w_1 \\ -sin\, x_1 - x_2^2 - x_4 - w_2 \\ -x_4 \\ 0 \end{bmatrix}, \quad \tau = \begin{bmatrix} 0 \\ 0 \\ u_1 \\ u_2 \end{bmatrix}. \tag{29}$$

Let define the vector of tracking errors $e(t, q) \in \mathbb{R}^m$ for the positioning control tasks as the difference between the output vector $y(q) \in \mathbb{R}^m$ and the vector of references $y_{ref}(t) \in \mathbb{R}^m$

$$e(t, q) = y(q) - y_{ref}(t). \tag{30}$$

The control objective is to force the system outputs to the integral sliding manifold

$$S = \left\{ s,\ q,\ \dot{q} \,\middle|\, \sigma(s, e, \dot{e}) = 0 \right\}, \quad s = \int_0^t e\, \mathrm{d}t, \tag{31}$$

where $\sigma \in \mathbb{R}^n$ is the sliding surface that provides relative degree one with respect to (w.r.t.) the control input τ for position control tasks. The vector functions y and y_{ref} in (30), and σ in (31) are supposed to be sufficiently smooth.

Notation 1: The Jacobian matrix $J_q^y \in \mathbb{R}^{m\times n}$ of vector y w.r.t. vector q is

$$J_q^y = \nabla y = \begin{bmatrix} \nabla y_1 \\ \vdots \\ \nabla y_m \end{bmatrix} = \begin{bmatrix} \frac{\partial y_1}{\partial q_1} & \cdots & \frac{\partial y_1}{\partial q_n} \\ \vdots & \ddots & \vdots \\ \frac{\partial y_m}{\partial q_1} & \cdots & \frac{\partial y_m}{\partial q_n} \end{bmatrix}. \tag{32}$$

The first step in the control design is to derive a stabilizing control for the nominal model of the system (27), usually called the equivalent control [3]. It describes the system motion in the sliding mode and ensures that the system trajectories will be confined to the sliding manifold (31) once it has been reached. The time derivative of the sliding surface is derived using (27), (30), (31) and (32)

$$\dot{\sigma} = \mathrm{J}_s^\sigma \cdot \dot{s} + \mathrm{J}_e^\sigma \cdot \ddot{e} + \mathrm{J}_{\dot{e}}^\sigma \cdot \ddot{e} \tag{33}$$

$$= \mathrm{J}_s^\sigma \cdot e + \mathrm{J}_e^\sigma \cdot \dot{e} + \mathrm{J}_{\dot{e}}^\sigma \cdot \left(\mathrm{J}_q^y \cdot \ddot{q} - \ddot{y}_{ref}\right) \tag{34}$$

$$= \mathrm{J}_s^\sigma \cdot e + \mathrm{J}_e^\sigma \cdot \dot{e} + \mathrm{J}_{\dot{e}}^\sigma \cdot \left[\mathrm{J}_q^y \cdot a_n^{-1}\left(\tau - \tau_{dis}\right) - \ddot{y}_{ref}\right]. \tag{35}$$

For the sake of simplicity, it is assumed in (35) that the second order derivatives $\partial^2 y_i/\partial q_j^2$ are equal to zero, for all $i = 1, \ldots, m$ and $j = 1, \ldots, n$, since the outputs of the position control tasks, in general, are linear functions of the state variables. Let us introduce a non-singular matrix function $\alpha = a_n \cdot \left(\mathrm{J}_{\dot{e}}^\sigma \cdot \mathrm{J}_q^y\right)^{-1}$, such that $\mathrm{J}_{\dot{e}}^\sigma \cdot \mathrm{J}_q^y$ is a non-singular $n \times n$ matrix. The equivalent control vector is derived to cancel the RHS of (35) in the absence of disturbances

$$\tau_{eq} = \alpha \cdot \left(\mathrm{J}_{\dot{e}}^\sigma \cdot \ddot{y}_{ref} - \mathrm{J}_s^\sigma \cdot e - \mathrm{J}_e^\sigma \cdot \dot{e}\right). \tag{36}$$

For the actual system (27) affected with disturbances τ_{dis}, two additional control terms $\hat{\tau}_{dis}$ and τ_v are included in the overall control τ

$$\tau = \tau_{eq} + \hat{\tau}_{dis} + \tau_v, \tag{37}$$

where $\hat{\tau}_{dis}$ is the RIC based control term for a lumped disturbance estimation. It aims to alleviate the chattering phenomenon by reducing the magnitudes of the sliding control vector τ_v. The main objective of the switching control term τ_v is to force the sliding mode motion toward the manifold (31) and to counteract the disturbance compensation error

$$\delta\left(\tau_{dis}, \hat{\tau}_{dis}\right) = \tau_{dis} - \hat{\tau}_{dis}, \tag{38}$$

rather than the lumped disturbance τ_{dis}. Thus, the overall control (37) should be able to stabilize the closed-loop system

$$a_n \ddot{q} = \tau_{eq} + \tau_v + \hat{\tau}_{dis} - \tau_{dis} \tag{39}$$

in the presence of modeling uncertainties, parameter variations and external disturbances.

Assumption 1: Assume that the lumped disturbance τ_{dis} is bounded such that

$$\left|\sigma^T \alpha^{-1} \tau_{dis}\right| \le \rho \left\|\sigma\right\|_2^2 + k_1 \left|\sigma^T \alpha^{-1} \hat{\tau}_{dis}\right| + k_2 \left|\sigma^T \alpha^{-1} \tau_v\right| \tag{40}$$

holds, where $\rho(t, q, \dot{q}) : [0, \infty) \times D \times D \to \mathbb{R}_0^+$ is a non-negative continuous function representing a disturbance magnitude, α is a non-singular matrix function, and $k_1,\ k_2 \in [0, 1]$ are constant parameters.

Remark 2: The only information one should know about the lumped disturbance τ_{dis} is the estimation (40), which does not require the function ρ to be small, but only to be known.

Assumption 2: The disturbance compensation error (38) is bounded by a non-negative constant δ_0, such that

$$\left\|\delta\right\|_1 \le \delta_0 \tag{41}$$

holds.

Notation 2: Let define a diagonal matrix $\eta_1(t, q, \dot{q}) = diag\left(\eta_{11}(t, q, \dot{q}), \ldots, \eta_{1n}(t, q, \dot{q})\right)$ of non-negative functions $\eta_{1i}(t, q, \dot{q}), \forall i = 1, \ldots, n$, and a non-negative scalar function $\eta_2(t, q, \dot{q})$, i.e. $\eta_{1i}, \eta_2 : [0, \infty) \times D \times D \to \mathbb{R}^+$.

Notation 3: Let define the vector $(\eta_1 * \sigma) \in \mathbb{R}^n$ of the convolutions $\eta_{1i} * \sigma_i$, for all $i = 1, \ldots, n$ and the vector $sgn\,\sigma \in \mathbb{R}^n$ of signs of the sliding surfaces σ_i as follows

$$\eta_1 * \sigma = \left[\eta_{11} * \sigma_1, \ldots, \eta_{1n} * \sigma_n\right]^T \tag{42}$$

$$sgn\,\sigma = \left[sgn\,\sigma_1, \ldots, sgn\,\sigma_n\right]^T. \tag{43}$$

Theorem 1: Consider the system (27) satisfying Assumptions 1-2. Assume that the corresponding internal dynamics of the system (27) is input to state (ISS) stable. If the control parameters η_1 and η_2 are defined such that

$$\left|\sigma^T (\eta_1 * \sigma)\right| \ge \rho \left\|\sigma\right\|_2^2 \tag{44}$$

$$\eta_2 \ge \beta\sqrt{n},\ \beta \ge 0 \tag{45}$$

hold, then the trajectories of the closed loop system will converge to the integral sliding manifold (31) in finite time by means of the control law

$$\tau = \tau_{eq} + \hat{\tau}_{dis} + \tau_v, \tag{46}$$

$$\tau_{eq} = \alpha \cdot \left(J_{\dot{e}}^\sigma \cdot \ddot{y}_{ref} - J_s^\sigma \cdot e - J_e^\sigma \cdot \dot{e}\right), \tag{47}$$

$$\hat{\tau}_{dis} = -\frac{\alpha}{1 - k_1}\left(\eta_1 * \sigma\right), \tag{48}$$

$$\tau_v = -\frac{\alpha}{1 - k_2}\,\eta_2\, sgn\,\sigma. \tag{49}$$

Remark 3: A non-negative constant β in (45) represents a converging rate to the sliding manifold (31).

Proof: For the system (39), let define a positive definite Lyapunov function

$$V = \frac{\sigma^T \sigma}{2},\ V(0) = 0. \tag{50}$$

The first order time derivative of (50) along the trajectories of the system (39) is expressed using (35) and (46)

$$\dot{V} = \sigma^T \dot{\sigma} = \sigma^T \alpha^{-1}\left(\tau_v + \hat{\tau}_{dis} - \tau_{dis}\right) \tag{51}$$

$$\le \sigma^T \alpha^{-1}(\tau_v + \hat{\tau}_{dis}) + \left|\sigma^T \alpha^{-1} \tau_{dis}\right|. \tag{52}$$

Applying (44)-(49) and the estimation (40) to (52) yields

$$\dot{V} \leq -\frac{\sigma^T(\eta_1 * \sigma)}{1-k_1} - \eta_2 \frac{\sigma^T \operatorname{sgn}\sigma}{1-k_2} + \rho \|\sigma\|_2^2 + \frac{k_1 \left|\sigma^T(\eta_1 * \sigma)\right|}{1-k_1} + \eta_2 \frac{k_2 \left|\sigma^T \operatorname{sgn}\sigma\right|}{1-k_2} \quad (53)$$

$$\leq -\left|\sigma^T(\eta_1 * \sigma)\right| + \rho \|\sigma\|_2^2 - \frac{\eta_2}{\sqrt{n}} \|\sigma\|_2 \quad (54)$$

$$\leq -\rho \|\sigma\|_2^2 + \rho \|\sigma\|_2^2 - \beta \|\sigma\|_2 = -\beta\sqrt{2V}, \quad (55)$$

since the following

$$\left|\sigma^T \operatorname{sgn}\sigma\right| = \|\sigma\|_1 \geq \frac{\|\sigma\|_2}{\sqrt{n}} \quad (56)$$

$$\sigma^T(\eta_1 * \sigma) = \left|\sigma^T(\eta_1 * \sigma)\right| \quad (57)$$

hold. The scalar function $\sigma^T(\eta_1 * \sigma)$ on the LHS of (57) is non-negative, i.e.

$$\begin{aligned}\sigma^T(\eta_1 * \sigma) &= [\sigma_1, \ldots, \sigma_n]\,[\eta_{11} * \sigma_1, \ldots, \eta_{1n} * \sigma_n]^T \\ &= \sum_{i=1}^{n} \sigma_i(\eta_{1i} * \sigma_i) = \sum_{i=1}^{n} |\sigma_i(\eta_{1i} * \sigma_i)| \\ &= \left|\sum_{i=1}^{n} \sigma_i(\eta_{1i} * \sigma_i)\right| = \left|\sigma^T(\eta_1 * \sigma)\right|, \end{aligned} \quad (58)$$

since the functions $\sigma_i(\eta_{1i} * \sigma_i)$ are non-negative for all $i = 1, \ldots, n$.

It can be observed from (55) that the function $\dot{V}$ is negative definite along the trajectories of the closed loop system (39). Applying the comparison lemma [42] to (55) yields

$$\|\sigma(t, q, \dot{q})\|_2 \leq \|\sigma(t_0, q_0, \dot{q}_0)\|_2 - \beta t, \quad (59)$$

which guarantees that the trajectories starting off the sliding manifold (31), i.e. $\sigma(t_0, q_0, \dot{q}_0) \neq 0$, will reach it in finite time. Otherwise, the system trajectories starting on the integral sliding manifold (31), i.e. $\sigma(t_0, q_0, \dot{q}_0) = 0$, will be confined to it for all future time, because leaving the manifold requires the function $\dot{V}$ to be positive, which is impossible regarding (55). Therefore, the system trajectories reach the positively invariant set (31) in finite time and remain inside thereafter. □

Corollary 1: The trajectories of the closed-loop system (39) converge asymptotically to the equilibrium if the lumped disturbance τ_{dis} is vanishing.

Proof: Combining the Cauchy-Schwarz and Young's inequalities

$$\left|\sigma^T(\eta_1 * \sigma)\right| \leq \|\sigma\|_2 \|\eta_1 * \sigma\|_2 \leq \|\eta_1\|_1 \|\sigma\|_2^2 \quad (60)$$

with the lower bound (44) yields

$$\rho \|\sigma\|_2^2 \leq \|\eta_1\|_1 \|\sigma\|_2^2, \quad (61)$$

or

$$\|\eta_1\|_1 \geq \rho. \quad (62)$$

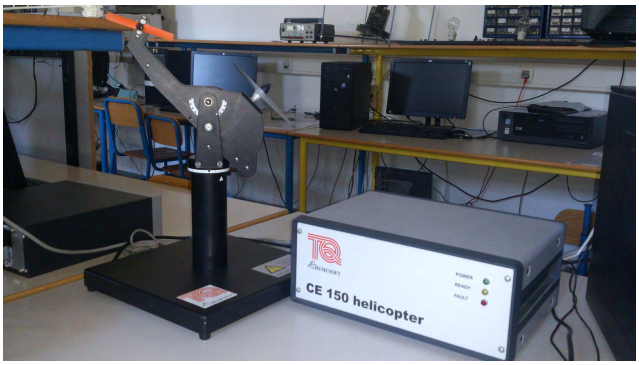

FIGURE 2. Laboratory helicopter system CE 150.

It follows from the results of Theorem 1 and (62) that the equilibrium point of the system (39) is asymptotically stable. □

Remark 4: The ultimate boundedness of the system trajectories is the best result that could be guaranteed if the generalized disturbance τ_{dis} is supposed to be non-vanishing [38].

Remark 5: If the control parameter η_1 of the RIC based control (48) is designed w.r.t. to (44), so the maximum value of the disturbance compensation error is δ_0, then the magnitude η_2 of the switching term (49) could be defined using (45) to dominate only over δ_0, instead of the whole disturbance τ_{dis}. Thus, the proposed SMRIC framework allows significantly lower magnitudes of the switching control vector and attenuation of the chattering effect.

Remark 6: The SMRIC scheme retains the nominal performance of the system, since the RIC based control term (48) behaves like a patch to the overall control, which does not operate in the absence of disturbances [36].

Remark 7: The estimation (40) does not require the lumped disturbance τ_{dis} to have constant steady-state values, or even to be continuous, but only to be bounded. Thus, the SMRIC approach has significantly relaxed constraints imposed on the mismatched uncertainties in comparison with the NDOB based SMC [15] and extended DOB based SMC [29].

IV. APPLICATION TO THE HELICOPTER SYSTEM CE 150

The laboratory helicopter CE 150 represents a highly nonlinear MIMO system with significant cross-couplings, thus imposing a challenge to a robust control design. Fig. 2 shows the main components of the helicopter system: the massive support, the rigid body with the ballast, two propellers driven by two DC motors, the power unit and the multifunctional card for data acquisition and implementation of the control algorithms. The small-scale helicopter CE 150 has 3 inputs: the main servomotor voltage u_1, the tail servomotor voltage u_2 and the additional servomotor voltage u_3 for moving the ballast along the longitudinal bar; and 2 outputs: the pitch (elevation) θ and the yaw (azimuth) ψ. The operational range of the helicopter inputs and outputs are listed in Tab. 2.

TABLE 2. Constraints for the helicopter input and output variables.

	Variable	Operational range
Inputs	u_1	$[0, 0.6]$
	u_2	$[-0.3, 0.3]$
	u_3	$[-1, 0]$
Outputs	θ	$[-45^\circ, 45^\circ]$
	ψ	$[-130^\circ, 130^\circ]$

A. MATHEMATICAL MODEL OF THE HELICOPTER DYNAMICS

This subsection presents a summary model of the helicopter CE 150, since the detailed dynamic model is already described in [37], [39], [40].

Fig. 3 shows the torques acting on the helicopter body. Considering the torques balance in the helicopter vertical plane, the elevation dynamics can be described as

$$a_\theta \ddot{\theta} = \tau_1 + \tau_{\dot{\psi}} - \tau_{f_1} - \tau_m - \tau_G, \tag{63}$$

$$\tau_{\dot{\psi}} = ml\dot{\psi}^2 \sin\theta \cos\theta, \tag{64}$$

$$\tau_{f_1} = C_\theta \operatorname{sgn}\dot{\theta} + B_\theta \dot{\theta}, \tag{65}$$

$$\tau_m = mgl \sin\theta, \tag{66}$$

$$\tau_G = K_G \dot{\psi} \omega_1 \cos\theta, \text{ for } \dot{\psi} \ll \omega_1, \tag{67}$$

where a_θ is the moment of inertia around the horizontal axis $\vec{\theta}$, τ_1 represents the moment of the main rotor, $\tau_{\dot{\psi}}$ is the centrifugal torque, m is the helicopter mass, l defines the distance between the horizontal axis $\vec{\theta}$ and the main servomotor axis $\vec{\omega}_1$, τ_{f_1} denotes Coulomb and viscous friction torques, B_θ and C_θ denote Coulomb and viscose friction coefficients for the elevation dynamics, respectively, τ_m is the gravitational torque, g stands for the gravitational acceleration, τ_G represents the gyroscopic torque, K_G is the gyroscopic coefficient and ω_1 represents the angular velocity of the main rotor.

The azimuth dynamics can be described using the torques balance in the horizontal plane of the helicopter

$$a_\psi \ddot{\psi} = \tau_2 - \tau_{f_2} - \tau_r, \tag{68}$$

$$\tau_{f_2} = C_\psi \operatorname{sgn}\dot{\psi} + B_\psi \dot{\psi}, \tag{69}$$

$$a_\psi = a_\theta \sin\theta, \tag{70}$$

where a_ψ is the moment of inertia around the vertical axis $\vec{\psi}$, τ_2 denotes the moment of the tail rotor, τ_{f_2} represents Coulomb and viscose friction torques, B_ψ and C_ψ denote Coulomb and viscose friction coefficients for the azimuth dynamics, and τ_r determines the helicopter cross-coupling dynamics, that is the reaction torque of the main servomotor w.r.t. the azimuth dynamics.

There is an unmodeled dynamics in (63)−(70), such as the main DC motor stabilizing torque, coupling effects between the tail rotor speed and the azimuth friction torque, variations in the air resistance, etc. Since the helicopter CE 150 construction does not allow measurement of the appropriate internal signals, the servomotors dynamics is approximated with the second order transfer function, the rotors torque is represented as the quadratic function of the angular velocity, and the empirical model of the cross-coupling dynamics is described with the first order transfer function [38]. The effects caused by unmodeled dynamics, as well as approximated dynamics of the helicopter are managed by the RIC structure in the control design. Unknown parameters of the helicopter model are identified using a genetic algorithm and presented in [39].

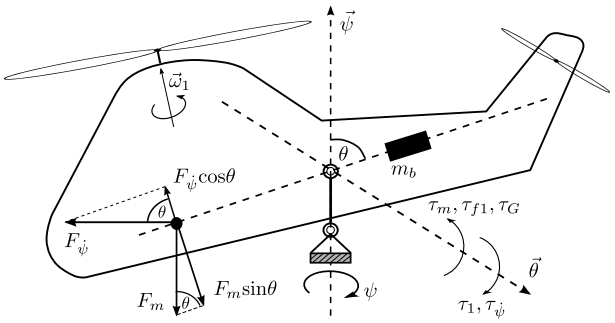

FIGURE 3. Torques acting on the helicopter body.

B. CONTROL DESIGN FOR THE HELICOPTER SYSTEM CE 150

The overall dynamics (63)−(70) of the helicopter CE 150 can be expressed using (27), introducing the substitutions

$$q = \begin{bmatrix} \theta \\ \psi \end{bmatrix}, \quad a_n = \begin{bmatrix} a_\theta & 0 \\ 0 & a_\psi \end{bmatrix}, \tag{71}$$

$$\tau = \begin{bmatrix} \tau_1 \\ \tau_2 \end{bmatrix}, \quad \tau_{dis} = \begin{bmatrix} \tau_{f1} + \tau_m + \tau_G - \tau_{\dot{\psi}} \\ \tau_{f2} + \tau_r \end{bmatrix}. \tag{72}$$

In order to provide the relative degree one ($r = 1$) from the control input τ to the helicopter output $y(q) = q = [\theta, \psi]^T$, the integral sliding surface is defined as

$$\sigma(t, q, \dot{q}) = \dot{e}(t, q) + \Lambda\, e(t, q) + \Gamma \int_0^t e(t, q)\, \mathrm{d}t, \tag{73}$$

where $\Lambda \in \mathbb{R}^{2\times 2}$ and $\Gamma \in \mathbb{R}^{2\times 2}$ are positive constant matrices, and the tracking error vector $e(t, q) \in \mathbb{R}^2$ is defined as $e(t, q) = q(t) - q_{ref}(t)$. Comparing the Laplace transforms of the disturbance attenuation control term (48) for $k_1 = 0$ and the RIC based control term in [34] yields

$$\eta_1 = \mathscr{L}^{-1}\left\{\frac{K(s)}{s}\right\}. \tag{74}$$

The overall control for the helicopter CE 150 follows from Theorem 1 (applying $k_2 = 0$)

$$\tau = a_n\left(\ddot{q}_{ref} - \Lambda\dot{e} - \Gamma e\right) - a_n \mathscr{L}^{-1}\left\{s^{-1}K(s)\sigma(s)\right\} - a_n \eta_2 \operatorname{sgn}\sigma. \tag{75}$$

Block diagram of the control law (75) is depicted in Fig. 4.

In order to increase stability margins and decrease rise and settling times of the helicopter output responses, the phase-lead compensator is employed

$$K(s) = \operatorname{diag}\left(K_{L1}\frac{T_{L1}s + 1}{\kappa_1 T_{L1}s + 1}, K_{L2}\frac{T_{L2}s + 1}{\kappa_2 T_{L2}s + 1}\right) \tag{76}$$

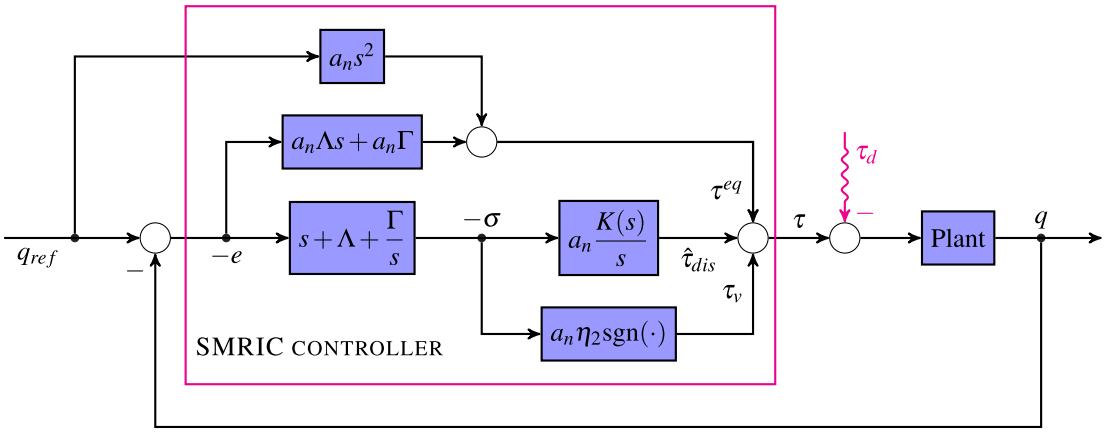

FIGURE 4. The proposed SMRIC scheme for output tracking of the laboratory helicopter CE 150. The ideal differentiator blocks s and s^2 are implemented using the real differentiator blocks.

where K_{L1}, K_{L2}, T_{L1} and T_{L2} are positive constants, $\kappa_1 = (1-\sin\phi_1)(1+\sin\phi_1)^{-1}$ and $\kappa_2 = (1-\sin\phi_2)(1+\sin\phi_2)^{-1}$ denote positive coefficients such that $\kappa_1, \kappa_2 \in (0, 1)$, while ϕ_1 and ϕ_2 represent positive phase contributions of the lead compensator (76) over the frequency ranges $[1/(\kappa_1 T_{L1}), 1/T_{L1}]$ and $[1/(\kappa_2 T_{L2}), 1/T_{L2}]$. Introducing substitutions $K_{L1} = a_\theta/(3T_1)^2$, $K_{L2} = a_\psi/(3T_2)^2$, $T_{L1} = 3T_1$, $T_{L2} = 3T_2$ and $\kappa_1 = \kappa_2 = 1/3$, the maximum phase contributions $\phi_{max1} = \phi_{max2} = 30°$ occur at the frequencies $\omega_{max1} = 1/(T_1\sqrt{3})$ and $\omega_{max2} = 1/(T_2\sqrt{3})$, and the RIC (76) can be represented by the third order low-pass filters within the DOB framework [34]

$$Q(s) = \mathrm{diag}\left(\frac{3(T_1 s)+1}{3(T_1 s)^3 + 3(T_1 s)^2 + 3(T_1 s)^2 + 1}, \frac{3(T_2 s)+1}{3(T_2 s)^3 + 3(T_2 s)^2 + 3(T_2 s)^2 + 1}\right). \quad (77)$$

V. SIMULATION AND EXPERIMENTAL RESULTS

The DOB based SMC [39], [40], as well as the RIC based SMC using decentralized [37] and centralized [38] approach have been applied to the helicopter CE 150 and reported the most promising tracking performance and robustness properties, in comparison with other control methods referenced therein. Here, the control performance of three control methods are compared through both simulation studies and experimental tests of the helicopter CE 150: the proposed integral SMRIC (I-SMRIC) with the phase-lead compensator (75), the RIC based I-SMC with the first-order low pass Q-filter [38] and the NDOB based I-SMC [15]. In order to implement the designed controllers, the real-time control scheme has been developed [37], [39], [40] using MATLAB (Simulink) toolkit software. The results are presented for the following values of the control parameters: $\Lambda = \mathrm{diag}(5, 7)$, $\Gamma = \mathrm{diag}(4, 6)$, $T = \mathrm{diag}(T_1, T_2) = \mathrm{diag}(2.5, 1.5)$, $\eta_2 = 6$ and $\beta = 10$ for the RIC based I-SMC law (75); $c_1^1 = 5$, $c_0^1 = 4$, $c_1^2 = 7$, $c_0^2 = 6$, $l_1 = [50, 0]$, $l_2 = [0, 50]$ and $\beta = 15$ for the NDOB based I-SMC; and the same values of the control parameters for the centralized RIC based I-SMC scheme as in [38]. The controller parameters are not optimized for the best control performance, but rather to illustrate the robustness properties of the control methods to external disturbances and parametric uncertainties.

A. SIMULATION RESULTS

In the simulation tests we imposed 30% uncertainties on the helicopter model parameters. We also simulated wind gusts by the low-frequency (1[rad/s]) periodic signal with a significantly strong magnitude (10[m/s]). It can be noticed from Fig. 5 that all three control techniques stabilize the helicopter outputs and maintain the reference attitudes over the whole domain. However, in comparison with the RIC based I-SMC and the NDOB based I-SMC laws, the I-SMRIC technique improved tracking performances of the helicopter CE 150 by decreasing rise and settling times, as well as the overshoots, especially in the pitch response (see the zoomed area in Fig. 5a) proved to be more complex from the control point of view. Since the imposed disturbances do not have constant steady state values, the proposed I-SMRIC method significantly reduced steady state errors in comparison with NDOB based I-SMC, even with the 30% lower magnitude β of the switching control term.

B. EXPERIMENTAL TESTBED RESULTS

The experimental results are conducted under the perturbation test. It is performed by moving the ballast along the longitudinal axis, thus introducing dynamical changes in the helicopter CoG. During the test, the ballast motion started from its default position, that is the middle of the longitudinal axis, towards one end of the axes to the other one, and so on. Fig. 6 depicts the tracking error responses of the helicopter outputs. It can be observed that both RIC based techniques, the RIC based I-SMC and the I-SMRIC, achieved lower overshoots and settling times in comparison with the NDOB based I-SMC, especially when the upper ultimate bound of the elevation angle is approached (see Fig. 6a).

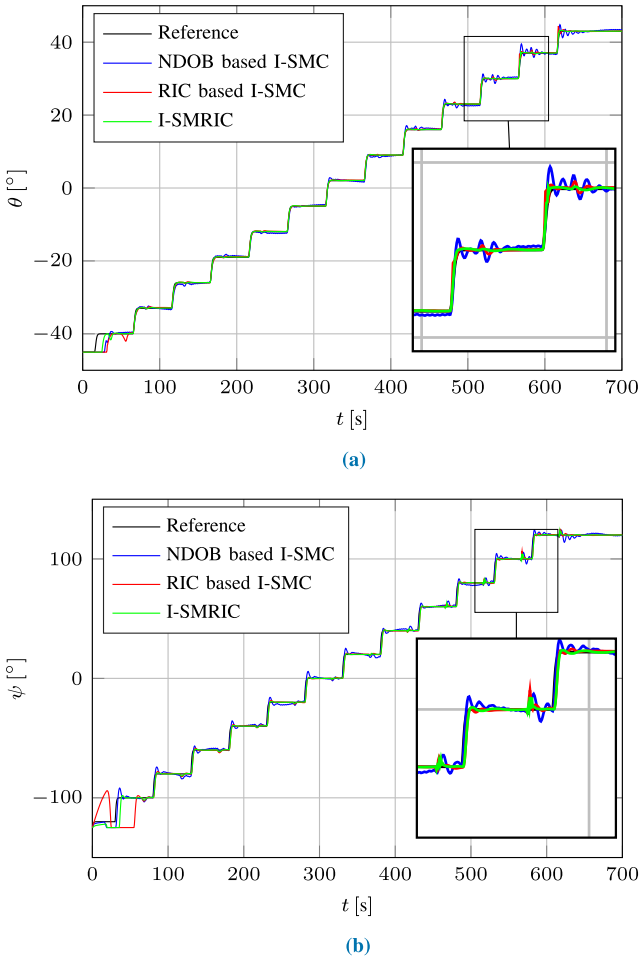

FIGURE 5. Helicopter output responses in the simulation mode. (a) Comparison of the elevation responses. (b) Comparison of the azimuth responses.

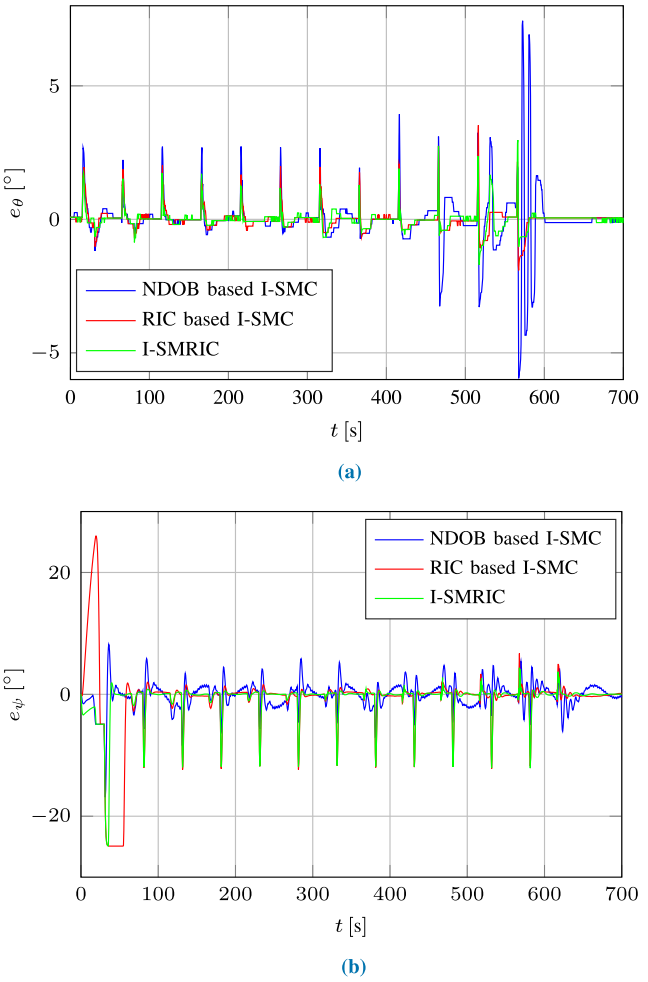

FIGURE 6. Tracking error responses of the helicopter outputs at the experimental setup. (a) Comparison of the elevation tracking error responses. (b) Comparison of the azimuth tracking error responses.

VI. CONCLUSION

By proposing a novel SMRIC method for a class of MIMO electromechanical systems, this paper has aimed to solve the traditional SMC issues: alleviation of the chattering, sensitivity to mismatched disturbances and nominal performance recovery. The SMRIC approach has extended an application area of the RIC scheme to a class of nonlinear systems, since the RIC stability analysis is originally introduced only for a class of linear systems [30]–[36]. It is proved that the SMRIC technique guarantees the finite-time convergence of the system trajectories to the generalized sliding manifold. It ensures the asymptotic stability of the equilibrium in the presence of vanishing mismatched disturbances, as well as uniformly ultimately boundedness of the system solutions in the presence of non-vanishing unmatched uncertainties. The SMRIC method has significantly relaxed constraints that are imposed on mismatched uncertainties, expanding a class of disturbances that could be subjected on the MIMO nonlinear systems. It does not require unmatched disturbances to be continuous as the DOB based SMC approach [29], or with constant steady-state values as the NDOB based SMC method [15], but only to be bounded. The excellent tracking performance and improved robustness of the I-SMRIC technique have been demonstrated in comparison with the outstanding NDOB based SMC algorithm [15] through both, simulation tests and experimental studies in the presence of additional parametric uncertainties and external disturbances (wind gusts and dynamical changes in the helicopter CoG) with non-constant steady-state values.

REFERENCES

[1] B. Draženović, "The invariance conditions in variable structure systems," *Automatica*, vol. 5, no. 3, pp. 287–295, 1969.
[2] V. Utkin, "Variable structure systems with sliding modes," *IEEE Trans. Autom. Control*, vol. 22, no. 2, pp. 212–222, Apr. 1977.
[3] A. Sabanovic, "Variable structure systems with sliding modes in motion control—A survey," *IEEE Trans. Ind. Informat.*, vol. 7, no. 2, pp. 212–223, May 2011.
[4] G. Bartolini, A. Pisano, E. Punta, and E. Usai, "A survey of applications of second-order sliding mode control to mechanical systems," *Int. J. Control*, vol. 76, nos. 9–10, pp. 875–892, Jan. 2003.
[5] S. K. Spurgeon, "Sliding mode observers: A survey," *Int. J. Syst. Sci.*, vol. 39, no. 8, pp. 751–764, Aug. 2008.
[6] A. Pisano and E. Usai, "Sliding mode control: A survey with applications in math," *Math. Comput. Simul.*, vol. 81, no. 5, pp. 954–979, 2011.

[7] J.-J. E. Slotine, J. K. Hedrick, and E. A. Misawa, "On sliding observers for nonlinear systems," *ASME J. Dyn. Sys., Meas., Control*, vol. 109, no. 3, pp. 245–252, 1987.
[8] J. Yang, S. Li, and W.-H. Chen, "Nonlinear disturbance observer-based control for multi-input multi-output nonlinear systems subject to mismatching condition," *Int. J. Control*, vol. 85, no. 8, pp. 1071–1082, 2012.
[9] K. D. Young, V. I. Utkin, and U. Ozguner, "A control engineer's guide to sliding mode control," *IEEE Trans. Control Syst. Technol.*, vol. 7, no. 3, pp. 328–342, May 1999.
[10] G. Golo and V. C. Milosavljević, "Robust discrete-time chattering free sliding mode control," *Syst. Control Lett.*, vol. 41, no. 1, pp. 19–28, 2000.
[11] C.-C. Cheng, M.-H. Lin, and J.-M. Hsiao, "Sliding mode controllers design for linear discrete-time systems with matching perturbations," *Automatica*, vol. 36, no. 8, pp. 1205–1211, 2000.
[12] Y.-J. Huang, T.-C. Kuo, and S.-H. Chang, "Adaptive sliding-mode control for nonlinearsystems with uncertain parameters," *IEEE Trans. Syst., Man, Cybern. B. Cybern.*, vol. 38, no. 2, pp. 534–539, Apr. 2008.
[13] X. Wei and L. Guo, "Composite disturbance-observer-based control and terminal sliding mode control for non-linear systems with disturbances," *Int. J. Control*, vol. 82, no. 6, pp. 1082–1098, 2009.
[14] Y. S. Lu, "Sliding-mode disturbance observer with switching-gain adaptation and its application to optical disk drives," *IEEE Trans. Ind. Electron.*, vol. 56, no. 9, pp. 3743–3750, Sep. 2009.
[15] J. Yang, S. Li, and X. Yu, "Sliding-mode control for systems with mismatched uncertainties via a disturbance observer," *IEEE Trans. Ind. Electron.*, vol. 60, no. 1, pp. 160–169, Jan. 2013.
[16] W.-H. Chen, "Nonlinear disturbance observer-enhanced dynamic inversion control of missiles," *J. Guid., Control, Dyn.*, vol. 26, no. 1, pp. 161–166, Jan. 2003.
[17] V. Utkin and J. Shi, "Integral sliding mode in systems operating under uncertainty conditions," in *Proc. 35th IEEE Conf. Decis. Control*, vol. 4, Dec. 1996, pp. 4591–4596.
[18] K.-S. Kim, Y. Park, and S.-H. Oh, "Designing robust sliding hyperplanes for parametric uncertain systems: A riccati approach," *Automatica*, vol. 36, no. 7, pp. 1041–1048, 2000.
[19] J.-L. Chang, "Dynamic output integral sliding-mode control with disturbance attenuation," *IEEE Trans. Autom. Control*, vol. 54, no. 11, pp. 2653–2658, Nov. 2009.
[20] W.-J. Cao and J.-X. Xu, "Nonlinear integral-type sliding surface for both matched and unmatched uncertain systems," *IEEE Trans. Autom. Control*, vol. 49, no. 8, pp. 1355–1360, Aug. 2004.
[21] F. Castanos and L. Fridman, "Analysis and design of integral sliding manifolds for systems with unmatched perturbations," *IEEE Trans. Autom. Control*, vol. 51, no. 5, pp. 853–858, May 2006.
[22] J. Yang, S. Li, J. Su, and X. Yu, "Continuous nonsingular terminal sliding mode control for systems with mismatched disturbances," *Automatica*, vol. 49, no. 7, pp. 2287–2291, 2013.
[23] A. Estrada and L. Fridman, "Quasi-continuous HOSM control for systems with unmatched perturbations," *Automatica*, vol. 46, no. 11, pp. 1916–1919, 2010.
[24] M. Basin, J. Rodriguez-Gonzalez, L. Fridman, and P. Acosta, "Integral sliding mode design for robust filtering and control of linear stochastic time-delay systems," *Int. J. Robust Nonlinear Control, IFAC-Affiliated J.*, vol. 15, no. 9, pp. 407–421, 2005.
[25] J. Zhang, X. Liu, Y. Xia, Z. Zuo, and Y. Wang, "Disturbance observer-based integral sliding-mode control for systems with mismatched disturbances," *IEEE Trans. Ind. Electron.*, vol. 63, no. 11, pp. 7040–7048, Nov. 2016.
[26] J. Yang, W.-H. Chen, and S. Li, "Non-linear disturbance observer-based robust control for systems with mismatched disturbances/uncertainties," *IET Control Theory Appl.*, vol. 5, no. 18, pp. 2053–2062, 2011.
[27] S. Li, J. Yang, W.-C. Chen, and X. Chen, "Generalized extended state observer based control for systems with mismatched uncertainties," *IEEE Trans. Ind. Electron.*, vol. 59, no. 12, pp. 4792–4802, Dec. 2012.
[28] J. Yang, A. Zolotas, W.-H. Chen, K. Michail, and S. Li, "Robust control of nonlinear MAGLEV suspension system with mismatched uncertainties via DOBC approach," *ISA Trans.*, vol. 50, no. 3, pp. 389–396, 2011.
[29] D. Ginoya, P. D. Shendge, and S. B. Phadke, "Sliding mode control for mismatched uncertain systems using an extended disturbance observer," *IEEE Trans. Ind. Electron.*, vol. 61, no. 4, pp. 1983–1992, Apr. 2014.
[30] B. K. Kim and W. K. Chung, "Performance predictable design of robust motion controllers for high-precision servo systems," in *Proc. Amer. Control Conf.*, vol. 3, Jun. 2001, pp. 2249–2254 vol.3.
[31] B. K. Kim and W. K. Chung, "Unified analysis and design of robust disturbance attenuation algorithms using inherent structural equivalence," in *Proc. Amer. Control Conf.*, vol. 5, Jun. 2001, pp. 4046–4051.
[32] B. K. Kim and W. K. Chung, "Advanced design of disturbance observer for high performance motion control systems," in *Proc. Amer. Control Conf.*, vol. 3, May 2002, pp. 2112–2117.
[33] B. K. Kim and W. K. Chung, "Performance tuning of robust motion controllers for high-accuracy positioning systems," *IEEE/ASME Trans. Mechatronics*, vol. 7, no. 4, pp. 500–514, Dec. 2002.
[34] B. K. Kim and W. K. Chung, "Advanced disturbance observer design for mechanical positioning systems," *IEEE Trans. Ind. Electron.*, vol. 50, no. 6, pp. 1207–1216, Dec. 2003.
[35] B. K. Kim, S. Park, W. K. Chung, and Y. Youm, "Robust controller design for PTP motion of vertical XY positioning systems with a flexible beam," *IEEE/ASME Trans. Mechatronics*, vol. 8, no. 1, pp. 99–110, Mar. 2003.
[36] B. K. Kim, W. K. Chung, and K. Ohba, "Design and performance tuning of sliding-mode controller for high-speed and high-accuracy positioning systems in disturbance observer framework," *IEEE Trans. Ind. Electron.*, vol. 56, no. 10, pp. 3798–3809, Oct. 2009.
[37] A. Salihbegovic, M. Hebibovic, and E. Sokic, "Synthesis of the integral sliding mode control and the robust internal-loop compensator for a class of nonlinear systems with matched uncertainties," in *Proc. 25th Int. Conf. Inf., Commun. Automat. Technol. (ICAT)*, Oct. 2015, pp. 1–8.
[38] A. Salihbegovic, "Multivariable sliding mode approach with enhanced robustness properties based on the robust internal-loop compensator for a class of nonlinear mechanical systems," in *Proc. Eur. Control Conf. (ECC)*, Jun./Jul. 2016, pp. 382–387.
[39] A. Salihbegovic, E. Sokic, N. Osmic, and M. Hebibovic, "High performance disturbance observer based control of the nonlinear 2DOF helicopter system," in *Proc. 24th Int. Conf. Inf., Commun. Automat. Technol. (ICAT)*, Oct./Nov. 2013, pp. 1–7.
[40] A. Salihbegovic and M. Hebibovic, "Attitude tracking of the small-scale helicopter system using disturbance observer based sliding mode control," in *Proc. 22nd Medit. Conf. Control Automat. (MED)*, Jun. 2014, pp. 1578–1583.
[41] J. Davila, L. M. Fridman, and A. Levant, "Second-order sliding-mode observer for mechanical systems," *IEEE Trans. Autom. Control*, vol. 50, no. 11, pp. 1785–1789, Nov. 2005.
[42] H. Khalil, *Nonlinear System*. Upper Saddle River, NJ, USA: Prentice-Hall, 2002.

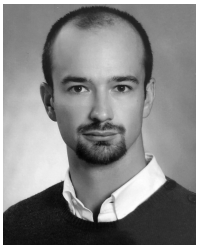

ALMIR SALIHBEGOVIC received the bachelor's and master's degrees from the Faculty of Electrical Engineering, University of Sarajevo, in 2008 and 2013, respectively, where he is currently pursuing the Ph.D. degree. He is currently a Research and a Senior Teaching Assistant with the Department for Automatic Control and Electronics, Faculty of Electrical Engineering, University of Sarajevo. His current research interests include fundamentals of automatic control, linear and nonlinear control systems, robust control, sliding mode control, disturbance observers, adaptive control, signal processing, artificial intelligence, mechatronic structures, and industrial automation.